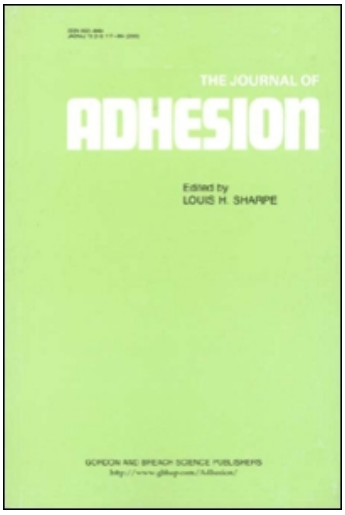

The Journal of Adhesion
Publication details, including instructions for authors and subscription information:
http://www.informaworld.com/smpp/title~content=t713453635

Production and Properties of Ejecta Released by Fracture of Materials

E. E. Donaldson[a]; J. T. Dickinson[a]; S. K. Bhattacharya[a]
[a] Department of Physics, Washington State University, Pullman, WA, U.S.A.

To cite this Article Donaldson, E. E. , Dickinson, J. T. and Bhattacharya, S. K.(1988) 'Production and Properties of Ejecta Released by Fracture of Materials', The Journal of Adhesion, 25: 4, 281 — 302
To link to this Article: DOI: 10.1080/00218468808071268
URL: http://dx.doi.org/10.1080/00218468808071268

J. Adhesion, 1988, Vol. 25, pp. 281–302
Reprints available directly from the publisher
Photocopying permitted by license only

Printed in the United Kingdom

Production and Properties of Ejecta Released by Fracture of Materials

E. E. DONALDSON, J. T. DICKINSON and S. K. BHATTACHARYA

Department of Physics, Washington State University, Pullman, WA 99164-2814, U.S.A.

(Received July 6, 1987; in final form January 29, 1988)

We have examined ejecta (particles in the size range 0.1 to 500 μm) which are released by fracture of a variety of materials. The ejecta from most non-metallic materials are electrically charged and frequently have high velocities. The amount of ejecta produced depends on the material and the conditions of fracture. For unfilled, glassy polymers the ejecta are produced in regions of fast-hackled fracture. Detailed measurements have been made on the ejecta mass and size distributions from the fracture of composites. From these measurements the total particle surface areas can be estimated and are found to be comparable to or greater than the cross-sectional area of the fractured samples. Thus, the ejecta should be a consideration in the analysis of surface energy and other parameters from fractographical analysis.

KEY WORDS Fracture; ejecta; fragmentation; polymers; composites; graphite.

I INTRODUCTION

The fracture of a range of materials in several fracture geometries causes the ejection of visible particles. For example, in previous studies of fracto-emission,[1] we noted that the front surfaces of our particle detectors (electron multipliers) accumulated tiny particles which clearly originated from the fracture zone. We decided to study the nature and origin of macroscopic particles arising from fracture, in particular those lying in size range from 0.1 to 500 μm.

We refer to these particles as *ejecta* following the precedent of Asay who applied this name to the particles ejected by shock waves.[2]

Ejecta from the fracture of materials have been studied previously. Sharpe and Logioco photographed ejecta arising from the failure of lap shear specimens made of polycarbonate bonded with an acrylic adhesive.[3] They pointed out that such ejecta could be of importance in any consideration of the fractography of the system; *i.e.*, missing components of the original fracture surface.

In shock loaded materials, Asay[2] measured the mass and velocities of the ejecta produced when the shock wave emerges from the back side of a sample. In the case of porous tungsten samples the ejecta, having a mass of many milligrams, were shown to have significant momentum. Grady and Benson fragmented aluminum and copper rings by loading them electromagnetically[4] so that they expanded radially, thereby failing in tension. These authors observed fragments in the size range from 0.1 to 1.0 g and found that the highest strain rates produced the smallest fragments.

In an unusual study involving considerably larger fragments, Kabo, Goldsmith, and Sackman[5] examined the impact of several kinds of massive projectiles on rocks. These investigators used photography to determine that the rock fragments produced by impact had velocities which ranged up to 350 m/sec. In one series of experiments 20 and 40 mm cannons were mounted on a U.S. Army M-47 tank and fired at the nearly vertical shale walls of an open pit mine. Some fragments were collected near the point of impact on polyethylene sheets spread on the floor of the mine. Other unanalyzed fragments were found within a radius of 100 m from the target.

Furthermore, there is considerable concern that ejecta may result in the formation of a belt of particles in orbit around the earth.[6] A large portion of this ejecta is produced from the breakup of earth satellites, explosions in space, and collisions between existing fragments and space vehicles. Satellites can be navigated to avoid the largest fragments, but smaller particles cannot be detected, and thus constitute a potential hazard to astronauts and space vehicles. As such particles continue to accumulate, an impassable belt may build up and render defense and scientific space systems inoperable in a few decades.

In addition to the above, ejecta from catastrophic fracture may

have other implications and, in some cases, cause injury. An example, eye injuries can result from the ejection of tiny chips of glass due to fracture of glass corrective lenses. In large accidents, the optical absorption from high volumes of ejecta could be a danger in certain circumstances. Also, the sudden release of large quantities of conducting fibers (*e.g.*, graphite) due to an airplane crash, etc., near high voltage transformers has been considered a possible hazard. In failure analysis, in the assessment of accidents, explosions, and criminal acts (where some form of fracture has occurred), examination of ejecta may provide additional clues as to the cause and/or sequence of events.

In the studies of fracture-induced ejecta presented here, we concentrate on the small fragments, arbitrarily choosing those with mass <0.1 mg. The larger fragments, few in number, are commonly known to fracture scientists and are clearly attributable to crack bifurcation. Here we describe the results of a survey designed to reveal what types of materials release microscopic ejecta due to fracture. This survey showed that ejecta are produced by the fracture of many materials in several fracture modes and/or specimen geometries. Subsequently, we examine in more detail some of the properties of ejecta from graphite-epoxy composites, including measurements of the total quantity of material released, the size distributions of the ejecta, the general morphology of the particles, the presence of electrical charge on the ejecta, and their kinetic energies. Finally, we also examine the ejecta from PMMA and unfilled epoxy in relation to features characterizing crack growth in these materials.

II EXPERIMENTS AND RESULTS

A. Survey of fracture induced ejecta

In order to determine the prevalence of ejecta, we began by fracturing a variety of pure and composite materials in several sample geometries. In many tests, a catcher of aluminum foil was placed under and around the fracture zone. After fracture, the larger fragments (>1 mm dimensions) were removed from the catcher and the remaining ejecta were weighed in a Cahn microbal-

ance. The masses given in Table I have been normalized by division by the original cross-sectional areas of the unfractured samples. In Table I, "visible" indicates that the collector showed ejecta visible to the naked eye under oblique lighting. The blank spaces in Table I

TABLE I
Observed ejecta and yields

	Yields $\mu g/mm^2$ Tensile Fracture	3 Point Flex
GLASSY MATERIALS		
Soda-Lime Glass Slide	0.80	1.0
PMMA	0.04	0.17
PS	0.11	0.09
Epoxy (EPON 828 Strong Samples)	30.0	0.63
Fused Silica		visible
Glass Fibers	visible	visible
Graphite Fibers	visible	visible
Epoxy (CIBA–GEIGY MY720 Cured with DDS)	visible	
PEEK	0.05	
COMPOSITE AND FILLED MATERIALS		
PS + Random Glass Fibers	2.15	0.13
Epoxy + Uniaxial Graphite Fibers (Thornel 300 in NARMCO 5208)		
Tension at 0° wrt Fibers		2.0
Tension at 90° wrt Fibers		0.5
Epoxy + Uniaxial Graphite Fibers (Fiberite 934)		
Tension at 0° wrt Fibers	visible	3.4
Tension at 90° wrt Fibers		1.8
Epoxy + Alumina Powder (EPON 828 filled with Alumina 1:1 by vol.)	2.5	0.13
PEEK + Carbon Fibers (80 μm length fibers, 30% by weight)	0.25	
CRYSTALLINE MATERIALS		
Silicon (100) Fract $\parallel$ to (110)		3.6
Fract 45° to (110)		5.4
Quartz		visible
Alumina		11.0
Sapphire		visible
MgO		visible
PZT		visible
LiF		visible
BN		1.0

indicate that no experiment was done for that particular material and geometry. Our general observations as a result of this survey are as follows:

1) A wide range of materials produce detectable or measurable ejecta when fractured in several different geometries.

2) The only exceptions to this general result are adhesives and elastomers with $T_g < T_{room}$. For example, unfilled and particulate filled elastomers yield almost no ejecta when fractured in tension at relatively low strain rates and at room temperature. Similarly, the peeling of simple adhesives produced no measurable ejecta at room temperature. To date, we have not investigated these materials at low temperatures (below T_g) or at very high strain rates; these conditions would be more likely to produce ejecta.

3) When nonisotropic materials were fractured in the "strong" direction they produced more ejecta than when they were broken in the "weak" direction. For example, for uniaxial graphite fiber-epoxy composites (Table I), the ejecta yield is at least twice as great when tension is *along* the fibers (0° orientation) *vs* normal to the fibers (90° orientation).

4) When graphite-epoxy composites were fractured in three-point bending geometry the ends split due to delamination. We found that the split ends of these samples which were far from the region of maximum tension but which were experiencing significant shear forces, were strong emitters of ejecta.

5) Unnotched samples (therefore, storing higher strain energy when stressed) produced more than ten times the mass of ejecta as compared to notched samples. The point is explored in more detail in Section E.

B. Properties of ejecta from graphite fiber-epoxy composites

A more detailed analysis was made of the ejecta from the fracture of uniaxial graphite fiber-epoxy composites which were relatively strong ejecta emitters. The specimens were made from Union Carbide Thornel 300 graphite fibers and NARMCO 5208 epoxy resin. Three-point bending experiments were done using 16-ply material having a sample cross-section of 2.4×6 mm. Tension

experiments used 2-ply samples of the same material with a cross-section of 0.35×6 mm with the fibers aligned either along the tension direction (0° orientation) or perpendicular to this direction (90° orientation). The thinner material was used for the tensile experiments due to limitations on our straining device.

Figures 1 and 2 show SEM photographs of the end and side views of this composite. Figure 1 is a polished and etched cross section of the specimen which reveals the distribution of the fibers in the matrix. Figure 2 is a side view of the fibers on a fracture surface of a 0° specimen loaded to failure in a three point flexure. For size reference note that the graphite fibers are approximately 7 μm in diameter. Figure 2 shows that after fracture, the graphite fibers and the columns of epoxy matrix are covered with epoxy scales which sometimes exhibit evidence of plastic flow, shown enlarged in Figure 3. These photographs suggest that the dominant composite failure mode is cohesive fracture through both matrix and fibers, although failure along the fiber-epoxy interface does occur to some extent.

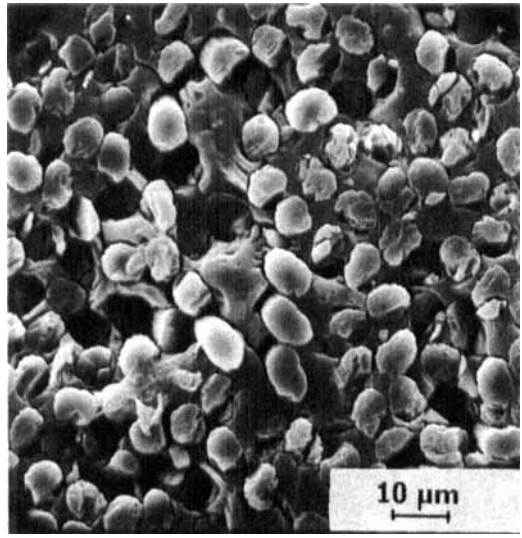

FIGURE 1 SEM photograph of graphite fiber-epoxy composite 16-ply. End view of fibers cut, polished, and lightly etched to free the fibers. The fibers are about 7 μm in diameter. Width of interstitial epoxy-filled channels 0 to 20 μm. Striations are visible on sides of some fibers.

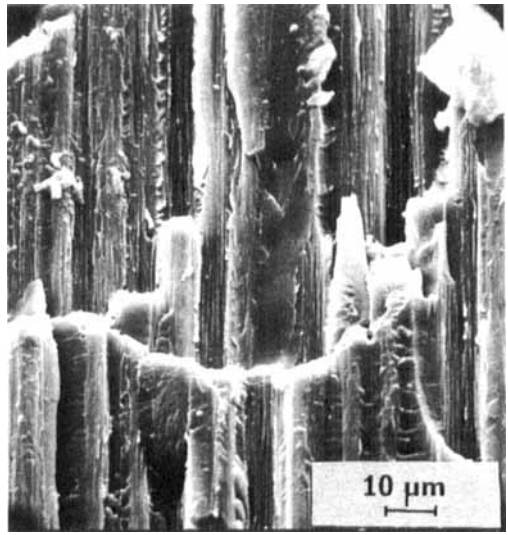

FIGURE 2 SEM photograph of fracture surface of graphite fiber-epoxy composite formed by three-point bending. Lengthwise striation of graphite fibers shown along with scales of adhering epoxy.

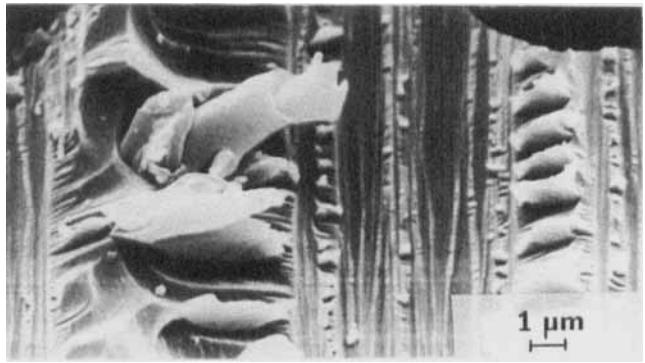

FIGURE 3 SEM photograph of surface like Figure 2 at higher magnification showing scales of epoxy and evidence of plastic flow.

Figures 4–6 are micrographs of the ejecta produced when the composite failed in three-point flexure. The optical micrograph in Figure 4 is a general view of ejecta and shows single graphite fibers, multiple fiber bundles, and smaller particles. It can be seen that some of the fibers appear clean and that others have scales or chips of the matrix attached. Figure 5 is a low-magnification SEM micrograph of typical ejecta, again revealing a range of ejecta morphology. Figure 6 shows a typical aggregation or clump of fibers and flakes of epoxy which presumably formed after ejection due to agglomeration of individual ejecta particles.

The ejecta morphology exhibited in these micrographs is consistent with the fracture surface shown in Figure 2; that is, the micrographs show pieces of epoxy adhering to the graphite fibers

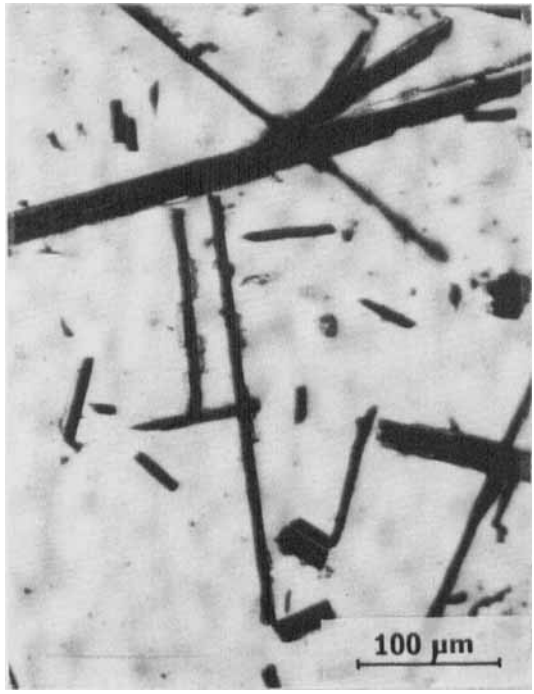

FIGURE 4 Optical micrograph of ejecta from three-point bending, 0° orientation fracture of graphite fiber-epoxy composite. Fiber lengths only were measured from such fields. Epoxy can be seen adhering to fibers. About 240×.

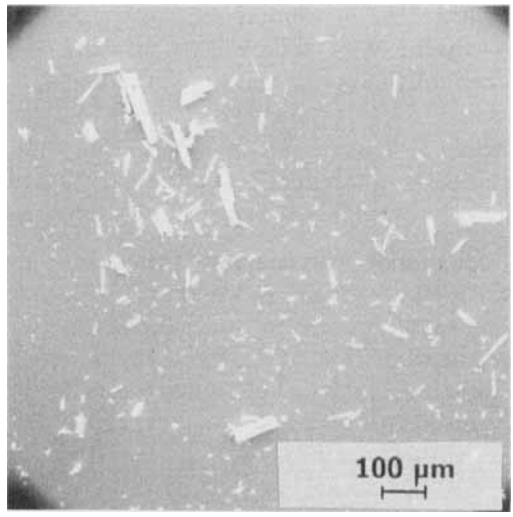

FIGURE 5 SEM photograph of ejecta from fracture as in Figure 4, showing single graphite fibers, graphite fiber bundles and clusters of small ejecta.

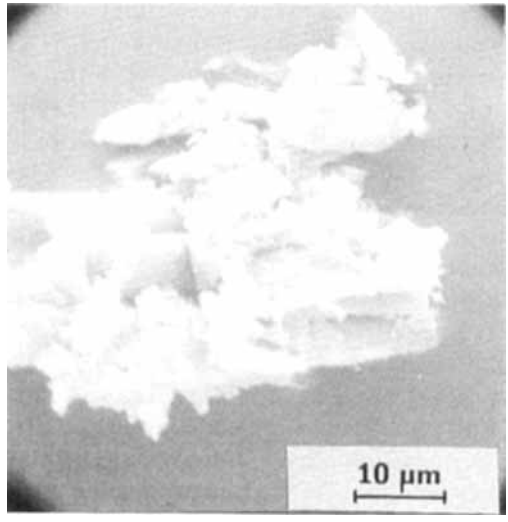

FIGURE 6 SEM photograph of ejecta from fracture as in Figure 4. Surfaces of fibers show clinging epoxy particles as small as 0.01 μm as well as scales of adhering epoxy. Presumably electrostatic forces form such clusters.

and also very finely divided epoxy particles. Again, these observations are consistent with failure that is largely *via* disruptive cohesive fracture of the epoxy and graphite fibers.

1. Total Mass of Ejecta. To determine the total mass of the ejecta, we placed an aluminum foil catcher under the sample and weighed the ejecta in a microbalance. Our findings were:

(a) For 90° orientation (fibers perpendicular to tensile axis) we collected, on the average, 0.5 μg/mm^2 of sample cross-secion. This is the "weak" direction of reinforcement.
(b) For 0° orientation (fibers parallel to tensile axis) we collected, on the average, 2 μg/mm^2 of sample cross-section. This is the "strong" direction of reinforcement and yields significantly greater quantities of ejecta.

2. Size and Morphology of Ejecta. Because the ejecta exhibit a diversity of composition, shapes, and sizes, a single size distribution which would represent all of these particles could not be obtained. We resolved the problem by counting all of the fiber-containing particles as single fibers. Separately we counted the other particles, which consisted *mostly* of epoxy, as matrix ejecta.

Under this simplifying classification we were able to measure the lengths of the graphite fibers and fiber bundles in an optical microscope because the graphite fibers are easy to identify by their black appearance. The length distributions of these graphite fibers and fiber bundles arising from four different fracture geometries are shown in Figure 7. In determining all of these size distributions we used a geometric progression of particle size ranges. The points plotted in each case show the percentage frequency distribution[7] *vs* particle size.

Because the ejecta composed of matrix material were very small and because they tended to form clusters or to cling to fibers, we produced SEM photographs which allowed the size of individual particles to be measured. Even though the matrix ejecta are very irregular in shape, an effective diameter was calculated for each particle by taking the average of its length and width. Figure 8 shows this effective diameter distribution for matrix ejecta resulting from four different fracture geometries.

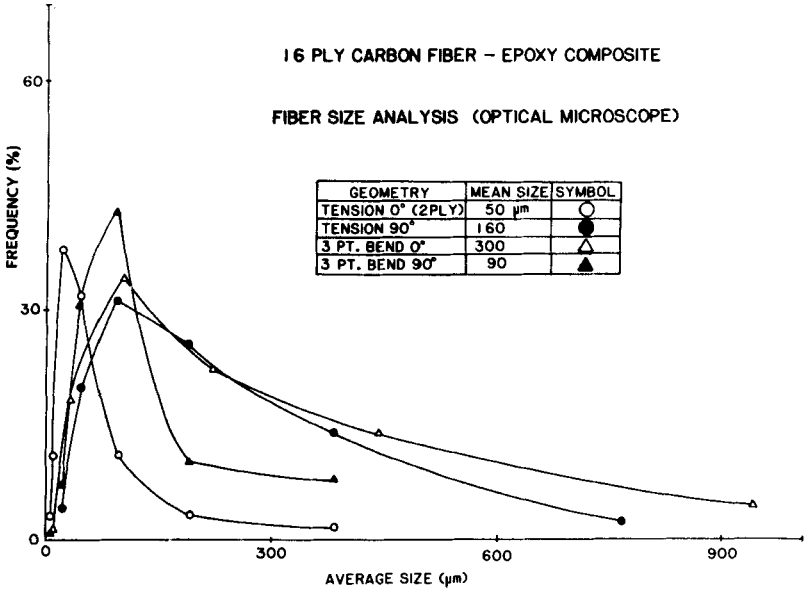

FIGURE 7 Size distributions (lengths) of fiber-containing ejecta from various fracture geometries for graphite fiber-epoxy composite obtained from optical microscopy.

The size distributions of the matrix particles in Figure 8 are quite similar for three point flexure and tensile fracture. This is probably due to the fact that in three-point bending, front layers of the composite fail in tension in a manner similar to tensile specimens, at the same local stress levels. Compression loading of the back side of the sample would play a small role in producing ejecta. In contrast, the fiber ejecta show size distributions dependent on fracture geometry (Figure 7). Note that for the fracture of the 2-ply material in tension the fiber ejecta are much shorter than for other geometries.

Examination of Figure 1 shows that the average width of the matrix-filled channels between fibers is 10 to 20 μm. However, the mean matrix ejecta size (from Figure 8) is only 1 μm. We know that the fibers in this composite are well bonded to the matrix because we find scales of epoxy attached to the graphite fibers following

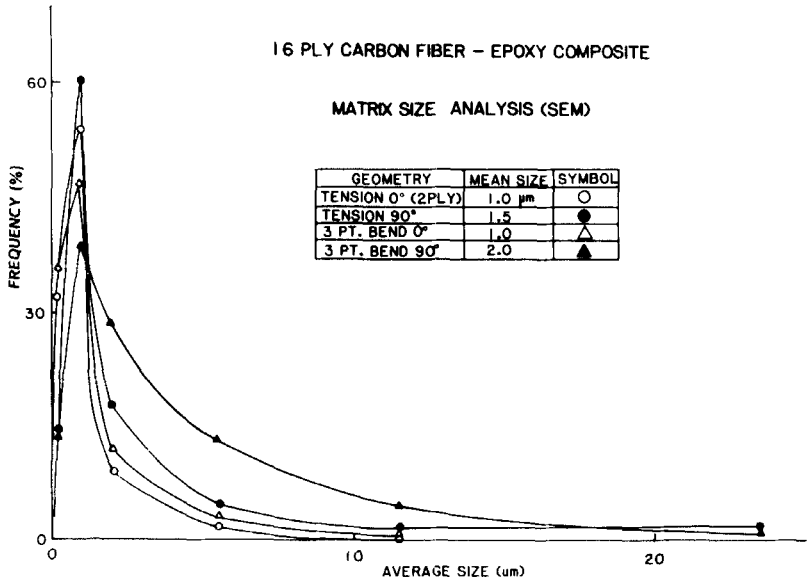

FIGURE 8 Size distributions of matrix ejecta from fracture of graphite fiber-epoxy composite obtained from the SEM.

fracture. In composites with well-bonded fibers, failure is initiated by fiber fracture. Apparently when these fibers fail they cause a very disruptive fracture of the matrix leading to the release of small matrix ejecta.

3. Surface Area of Ejecta. Having obtained the total mass and size distribution of the ejecta, we can estimate the total particle surface area for two extreme cases where we assume that all of the ejecta are matrix particles or that all of the ejecta are fiber particles. Let us examine the case of "all matrix" particles and choose the size distribution from three-point bending and 0° orientation of fibers (Figure 8). Assuming that the particles are spheres, the calculated specific surface area of the ejecta is $8.2 \times 10^5\ \text{mm}^2/\text{g}$. Table I shows an average of $15\ \mu\text{g}$ of ejecta from the fracture of such a sample with a cross-section of $7.35\ \text{mm}^2$. This quantity of ejecta would therefore have a surface area of at least $12\ \text{mm}^2$, which is comparable to the sample's cross-section.

A different result is calculated in the "all fiber" assumption. Because the specific surface area of ejecta in the form of fibers (assumed to be smooth cylinders) is about 5×10^4 mm^2/g, the same mass of ejecta would have an area of only 0.1 mm^2 if composed solely of fibers.

The assumptions made in the calculated surface areas for ejecta from graphite fiber-epoxy should in most cases lead to underestimates. As evidence, we first note that the SEM photographs show that the ejecta are not cylindrical and spherical in shape but are extremely rough and irregular and therefore have surface areas considerably larger than we calculate. Second, the total ejecta mass measurements are low because some of the high energy ejecta components escape collection. Finally, as we later describe, the trapping of ejecta in and around the crack occurs; *i.e.*, considerably more ejecta are created than released. All of these effects conspire to guarantee that the calculated areas are much lower than the actual areas.

C. Size distributions of ejecta from fracture of filled and unfilled PEEK

For a comparison with the results reported under Section B, we measured the total mass and the size distribution of ejecta arising from the tensile fracture of polyether ether ketone (PEEK). This material was originally formed by injection molding PEEK either unfilled or filled 30% by weight with short carbon fibers averaging 80 μm in length. Dog bone shaped samples were tested in tension.

Figure 9 is a plot of the size distribution of ejecta from the PEEK composite. Matrix ejecta from filled or unfilled PEEK have a mean diameter of 10 μm which is about an order of magnitude larger than the diameter of epoxy matrix ejecta (Figure 8). This can be attributed to the greater fracture toughness of PEEK in comparison to epoxy. We note that the mean length of the fiber ejecta from the PEEK composite was approximately 60 μm which is very close to the mean length of the original fibers. Thus, the release of essentially unbroken fibers upon fracture is due to the fact that these fibers are shorter than the criticial length associated with this particular PEEK/fiber interface.

Further evidence of a fairly weak interface was seen in SEM

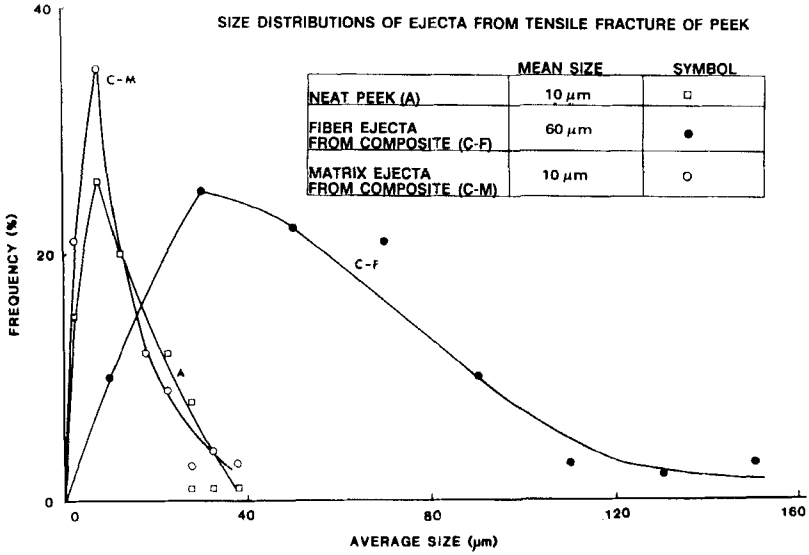

FIGURE 9 Size distributions of ejecta produced by tensile fracture of neat PEEK (curve A) and carbon fiber-PEEK composite (curve C–F for fibers and curve C–M for matrix ejecta).

photographs (not included) which show extensive fiber pullout during fracture of the PEEK composite. Thus, the weaker interface and tougher matrix make the fracture of carbon fiber-PEEK composite differ greatly from the failure of the epoxy composite.

D. Studies of electrical charges on ejecta

As we have noted earlier, we frequently found the fine ejecta particles clumped together in the form of large aggregates (*e.g.*, see Figure 6) suggesting that perhaps electrostatic forces were present. {A dramatic example of the aggregation of ejecta particles was experienced by those of us in Eastern Washington on May 18, 1980, a few hours after the eruption of Mt St. Helens. The ash created during the rhyolitic explosion which began falling in Pullman, Washington approximately 6 hours after the eruption was highly

aggregated, probably due to electrostatic attraction of the charged particles.[8]}

We examined the electric charge on fracture-induced ejecta in two different ways. In the first experiments we fractured composite specimens in tension between parallel vertical plates at potentials ± 2 kV, respectively. The plates each had an area of 15 cm^2 and they were separated by 2.4 cm creating a nearly uniform field to minimize polarization forces due to field gradients. Most of the ejecta experienced significant deflection and were collected on the plates. We sought but did not find any segregation of particular types of particles by charge sign; *i.e.*, fiber fragments were not separated from the matrix fragments on oppositely charged plates. This indicates that the ejecta composed primarily of matrix material or primarily of fiber material carry charge of either sign. Such a mixture of charge would encourage the aggregation or the clumping observed.

We also used three-point flexure to launch ejecta toward metal collector plates connected to an electrometer thereby measuring the total net charges on the ejecta. We found that individual ejecta or ejecta showers usually carried net charges of approximately 10^{-14} C and that net integrated charge on ejecta produced by the complete fracture of a sample several mm^2 in cross-section was in the range of 10^{-13} to 10^{-12} C. It should be emphasized that the detection of charges of both *signs* implies that the quantity of charge of each *sign* is likely to be considerably larger than the *net* value and that larger individual ejecta also carry patches of charge of both signs.

We might expect that the ejecta should be charged for a number of materials. When fracture occurs in piezoelectric materials, those containing a high density of charged point defects, and in specimens involving interfaces between dissimilar materials, we find that the newly created surfaces contain patches of $\pm$charge. This charge separation is particularly intense in the interfacial failure case, *e.g.* graphite and epoxy. Electrostatic discharges which occur during fracture frequently redistribute the charges in a variety of sign/density patches. Thus the ejecta can carry substantial charges of either sign. It is likely that electrostatic forces due to these charge patches play a role in the subsequent behavior and trajectories of the ejecta as well, although the kinetic energies of the ejecta come predominantly from the release of mechanical energy.

E. Velocity of ejecta

When uniaxial graphite fiber-epoxy composites are deformed in three-point flexure (with the fibers aligned along the tensile direction), the rapid failure of the outer plies is accompanied by an easily detectable acoustic emission (AE) burst. Thus an AE transducer can be used to detect the time these failure events occur to within a few microseconds. The charged ejecta which are released at fracture can be made to pass through two parallel grids where they induce detectable electrical signals in the form of pulses. We used the AE signal to start a time measurement and the electrical pulses to signal the arrival of ejecta at the grids. The signal from the first grid told us that the ejecta are released in a short time ($t < 1$ ms) after the fracture event and the signals from the first and the second grids told us that at least some ejecta travel at 50 m/s in air. Calculations based on Stokes,[9] law show that small spherical particles with diameters less than 5 μm would travel horizontally less than 1 cm in still air even if launched at initial speeds of 100 m/sec. Lower speeds or irregular shapes would result in a smaller range. Thus, the charged ejecta whose velocity were measured, must necessarily have been the larger fragments.

In spite of this air drag, one particularly strong epoxy sample produced ejecta with sufficient kinetic energy to make 50 visible indentations in the aluminum foil (0.015 mm thick) which we used as a catcher, demonstrating that these fragments can have considerable momentum.

F. Correlation of ejecta with fracture surface roughness in glassy polymers

In glassy materials, the nature of the fracture surfaces created is governed by the crack velocity. Slow crack growth produces smooth mirror-like surfaces; intermediate speed produces "mist" or lightly rippled surfaces; fast fracture produces very rough or "hackled" surfaces which result from crack bifurcation and branching.[10–15] When we examined the ejecta from PMMA and neat epoxy [Epon 828/Z Hardener] under a stereo microscope we identified particles in the shape of flakes and fibrils and saw other finely divided unresolved material. The hackled fracture surfaces of PMMA and

epoxy displayed potential ejecta having a similar appearance in a wide range of sizes, shapes, and strengths of attachment to the surface. A typical fast fracture surface for an unfilled epoxy showing these surface features is seen in Figure 10. We found that some of the particles were very loosely attached and could be dislodged by a blow to the back of the sample. These loose particles are ejecta which were trapped in the crack and remain bound to the surfaces. More tightly attached particles could be lifted off with adhesive tape. Even after tape had been peeled from the fracture surfaces they continued to hold flakes and fibrils which were firmly attached by one end.

A related observation was made on tensile fracture specimens of center notched samples of PMMA. Following the fracture, we microscopically examined the smooth faces of the sample adjacent to a fresh crack (*i.e.*, in the region of the dashed lines in Figure 11). Electrostatic charges on the ejecta and/or the surfaces caused the ejecta to be attracted to and captured by these surfaces. These finely divided ejecta were always concentrated near the rough or hackled fracture region, whereas very few ejecta were found near the mirror surfaces.

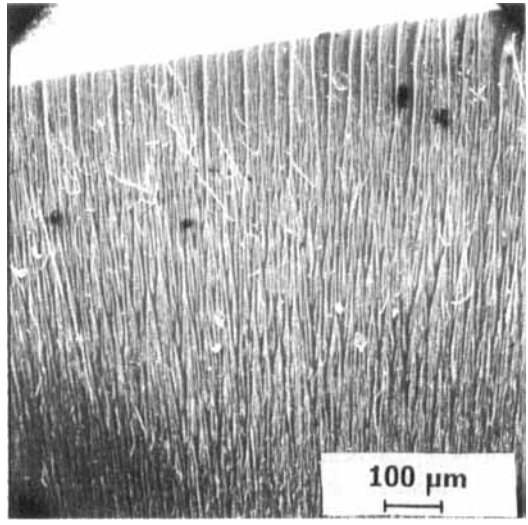

FIGURE 10 SEM photograph of fast tensile fracture surface of unfilled epoxy showing flakes and fibrils.

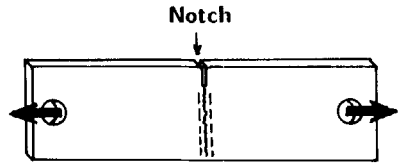

FIGURE 11 Sketch of PMMA tensile fracture sample showing region where ejecta were examined microscopically.

The above observations indicate a clear positive correlation between ejecta and hackled fracture. To provide further evidence of this association we weighed the ejecta produced by fracture initiated under different conditions. For example, unnotched tensile samples of epoxy were made with a smoothly tapered central section so that they would have little stress concentration and high elastic energy. Such samples were of high strength and they fractured by rapid crack growth producing very rough, hackled fracture surfaces. Notched samples were prepared with cuts made by broad and narrow saw blades. These notches caused higher stress concentration with failure at less elongation. This resulted in slower crack growth and smooth fracture surfaces. We cleaned the samples before fracture to remove chips or dust caused by shaping them. Because manipulation of the samples produced surface charge, we electrically neutralized them by brief exposure to the plasma above a propane flame just before they were tested, thereby reducing electrostatic retrapping of the ejecta.

The fracture of unnotched samples always produced rough hackled surfaces and more than 30 $\mu g/mm^2$ of ejecta (after the very large fragments were removed). In contrast, fracture of the samples with narrow saw notches produced smooth surfaces with much less total ejecta mass. The weakest samples with narrowest saw notches produced only 0.5 $\mu g/mm^2$ of ejecta, all of which were very small particles. Samples with wider saw notches produced an intermediate quantity of ejecta, averaging 1.3 $\mu g/mm^2$ of surface area. Thus, for glassy polymers such as PMMA, conditions encouraging fast crack propagation clearly encourage ejecta production. In viscoelastic materials, this would correspond to more brittle-like behavior. Therefore, we anticipate that lower temperature fracture and/or high strain rate loading of polymers, including elastomers, would enhance the production of ejecta.

G. Mechanisms for fracture induced ejecta

During rapid crack growth in glassy polymers, microcracks and voids form ahead of the crack tip. As the crack tip advances, the crack may branch or bifurcate along these microcracks.[11–15] Similarly, in inorganic materials such as glass, ceramics, and even single crystal brittle materials, such bifurcation can occur.[16] The multiple cracks may grow around large or small regions of the sample frequently arresting a small distance from the dominant crack. Thus free, lightly bound, and securely attached flakes or projecting structures are produced on the fracture surfaces. In polymers, material between microcracks may still remain under tension and be drawn plastically to produce fibrils which are frequently observed in the region of hackled fracture. In general, the fracture of brittle materials can produce a variety of particle-like protuberances in a number of shapes and sizes with varying degrees of attachment to the surfaces ranging from completely free to firmly bound. Similarly, in composites, the inhomogeneities cause crack paths to have extremes of crack bifurcation and branching, again creating numerous "near fragments" attached to the surface.

When a material is fractured there is a sudden release of strain energy. This sends mechanical release waves toward the gripped ends of the sample where they reflect back to the fracture zone. Fragments on the fracture surfaces which are partially detached by crack bifurcation can be ejected with momentum imparted by the wave.

Choosing PMMA as a model material and a sample size of a few mm in length, the wave would return to the fracture surfaces in 1 to 10 μs. We can write the characteristic equation for small amplitude acoustic waves in the form:[17]

$$\Delta u = \frac{\Delta p}{\rho c}$$

where Δu is the particle velocity and Δp the pressure increase produced when the material fails. We set Δp equal to the tensile stress of PMMA (~60 MPa). For the density we take 1.2×10^3 kg/m^3, and for the speed of sound, $c = 2500$ m/s. The calculated particle velocity, Δu, is then 20 m/s. When the reflected wave returns to the fracture surface, the free surface velocity is twice this

value, *i.e.*, 40 m/s. Assuming perfect coupling between the surface and partially attached fragments, the resulting ejecta could have final velocities of this magnitude. Focusing of the mechanical waves could produce even higher ejecta velocities, for example, at edges, corners, and other anisotropic features. This calculated velocity is consistent with the velocities of larger ejecta which we report above.

Only some of these released particles actually escape with these higher velocities. Others undergo wall collisions inside the crack and are trapped at the walls by electrostatic or van der Waals forces, and are frequently observed under the microscope. One would expect that electrostatic attraction and/or repulsion caused by patches of charge would also play a role in altering the trajectories of ejecta.

III CONCLUSIONS

Fracture-induced ejecta are produced when a variety of materials are broken in several modes of fracture. In a preliminary survey we have identified only a few materials such as elastomers and simple adhesives which do *not* produce observable fracture-induced ejecta at room temperature. Within a class of materials, the strongest samples yield the greater mass of ejecta. A geometry or a material which stores greater amounts of strain energy before failure will produce the greater mass of ejecta, emphasizing the importance of ejecta in the failure of strong and/or tough materials. Reinforced materials such as the graphite epoxy composite are copious sources of ejecta due to the high strain energies stored in the fibers.

The surface area of fracture-induced ejecta may be greater than the cross-sectional area of the fractured sample and thus ejecta should be considered in any description of fracture for most materials. High strength materials yield the most finely divided ejecta with high surface areas.

The ejecta from the nonmetallic materials and composites were found to be highly charged. One interesting question arises concerning the role such ejecta might play in inducing electrical breakdown if a fracture event occurred near high voltage gaps.

The relatively prompt release of the ejecta and the observed

velocities are consistent with a mechanism involving the reflection of the release wave created during fracture. The reflected wave imparts to the free surface a particle velocity which can couple mechanically to semi-attached fragments and thereby release them. Corners and edges are likely points of higher amplitude waves and therefore higher particle velocities.

When pure polymers fracture in tension the ejecta arise primarily from the regions corresponding to hackled surfaces. These surfaces contain numerous "chunks" which are more likely to be released. In a viscoelastic material, these hackled regions correspond to more brittle-like, higher velocity fracture. We anticipate that low temperature fracture and/or high strain rate loading would enhance the production of ejecta. It should be emphasized that the degree of crack bifurcation and branching is expected to increase with the total strain energy released during fracture. Likewise, the amplitude of the reflected waves would increase with the strain energy stored in the specimen. Therefore, one would expect a strong correlation between strain energy and quantity of ejecta released. Furthermore, any fractographic analysis of surface energy must take into account the fact that a large portion of the surface area carried away by the ejecta is created at the time of fracture and should therefore be included.

In summary, this study of fracture-induced ejecta has demonstrated their widespread occurrence and has provided intial information about ejecta morphology, size distributions, electrical charge, and velocity.

Acknowledgements

We wish to thank G. R. Fowles and Les Jensen, Washington State University, for helpful discussions and assistance in this work. We also thank Howard Nelson, NASA-Ames Research Center, for supplying the graphite-epoxy samples and Clarence Wolf, McDonnel Douglas Corporation, for supplying the PEEK samples. This work was supported by the McDonnell Douglas Independent Development Fund and the Washington Technology Center.

References

1. J. T. Dickinson, L. C. Jensen, and A. Jahan-Latibari, *J. Vac. Sci. Technol.* **A2,** 1112 (1984); J. T. Dickinson, A. Jahan-Latibari, and L. C. Jensen, in *Molecular*

Characterization of Composite Interfaces, N. G. Kumar and H. Ishida, Eds. (Plenum, New York, 1985), p. 111.
2. J. R. Asay, *J. Appl. Phys.* **49,** 6173 (1978); J. R. Asay, L. P. Mix, and F. C. Perry, *Appl. Phys. Lett.* **29,** 284 (1976).
3. L. H. Sharpe and J. W. Logioco, unpublished work.
4. D. E. Grady and D. A. Benson, *Exptl. Mech.* **13,** 393 (1983).
5. M. Kabo, W. Goldsmith, and J. L. Sackman, *Rock Mechanics* **9,** 213 (1977).
6. Comment by E. Marshall, *Science* **230,** 424 (1985).
7. T. Allen, *Particle Size Measurement,* 2nd edition (Chapman and Hall, London, 1975) Chapt. 4.
8. R. K. Sorem, *J. Volcan. Geotherm. Res.* **13,** 63 (1982).
9. E. H. Kennard, *Kinetic Theory of Gases* (McGraw-Hill, New York, 1938), p. 309.
10. H. H. Kausch, *Polymer Fracture* (Springer-Verlag, Berlin, 1978), pp. 300–306.
11. K. Ravi-Chandar and W. G. Knauss, *Internat. J. Fract.* **26,** 65 (1984).
12. W. G. Knauss and K. Ravi-Chandar, *ibid.* **27,** 127 (1985).
13. R. J. Morgan, J. E. O'Neal, and D. B. Miller, *J. Mater. Sci.* **14,** 109 (1979).
14. A. B. J. Clark and G. R. Irwin, *Exptl. Mech* **6,** 321 (1966).
15. C. J. Phillips in *Fracture: An Advanced Treatise* H. Liebowitz, Ed. (Academic Press, New York, 1972), Chap 1, sec IX.
16. B. R. Lawn and T. R. Wilshaw, *Fracture of Brittle Solids* (Cambridge University Press, Cambridge, 1975), pp. 100–105.
17. R. Courant and K. O. Friedrichs, *Supersonic Flow and Shockwaves* (Interscience Publishers, NY, 1948), p. 82.